

Fine resolution drop-on-demand electrohydrodynamic patterning of conductive silver tracks on glass substrate

Khalid Rahman · Kamran Ali ·
Nauman M. Muhammad · Myung-taek Hyun ·
Kyung-hyun Choi

Received: 22 June 2012 / Accepted: 9 September 2012 / Published online: 25 September 2012
© Springer-Verlag Berlin Heidelberg 2012

Abstract This paper presents the fine resolution printing of the silver patterns on the thick glass substrates, deposited through drop-on-demand electrohydrodynamic jetting by applying the pulsed voltage. The patterning is performed by ejecting ink containing silver nanoparticles through a 10 μm internal diameter glass capillary. The variations in patterns sizes are studied by changing the operating parameters and after sintering of deposited patterns on a 500 μm thick glass substrate. The minimum droplet diameter achieved is approximately 3.6 μm after the sintering process, which is 2.78 times smaller than the size of the capillary's internal diameter. The patterns are formed by suitable overlapping of droplets by adjusting the substrate speed and minimum pattern width achieved is 6.5 μm , which is the major attraction of electrohydrodynamic printing technology. The functionality of the deposited silver patterns is measured through I–V curve and shows linear Ohmic behavior with good resistivity. The experimental results indicate that the electrohydrodynamic printing can be used for fabricating fine resolution patterns of conductive tracks on thick substrate for printed electronics applications.

1 Introduction

There has been advancement in the field of inkjet printing beyond the conventional digital graphic arts printing [1]. Inkjet printing has been widely used to deposit various functional materials for fabrication of devices or device components in printed electronics [2–4] and bioapplications [5], etc. The inkjet based deposition has various advantages in flexibility of patterns to deposit, less material wastage, and can be scalable for large area fabrication. Conventional inkjet printing systems use thermal or acoustic energy to push the liquid from the nozzle for droplet generation. But these conventional inkjet printing systems have certain limitations, such as the thermal problem due to heating and cannot produce droplets smaller than the nozzle diameter apart from the limitation of materials to be deposited [6]. The conventional inkjet printing methods can typically produce the pattern size of 20–30 μm [7]. In order to achieve these resolutions or to minimize the feature size through conventional inkjet printing, substrate modification/treatment is necessarily required to modify the droplet and substrate interaction or printing on prepatterned or textured substrates to restrict the pattern size. In case of aqueous inks, the drop size is twice the droplet diameter ejected from the nozzle [8].

In order to reduce the pattern size, many researchers are focusing on the electrohydrodynamic jet based printing method. Electrohydrodynamic jet printing uses electric field by overcoming the surface tension to pull the liquid from the nozzle opening to deposit the material on the substrate rather than pushing the liquid as in case of conventional inkjet printing [9]. Due to pull of the liquid, electrohydrodynamic printing can produce smaller size patterns as compared to the nozzle diameter. Depending on the applied electric field (DC or pulse voltage), electrohydrodynamic jet printing can be continuous [10–12] or drop-on-demand [13–15]. Both

K. Rahman · K. Ali · N.M. Muhammad · K.-h. Choi (✉)
Department of Mechatronics Engineering, Jeju National
University, Jeju 690-756, Korea
e-mail: amm@jejunu.ac.kr

K. Rahman
Faculty of Mechanical Engineering, Ghulam Ishaq Institute of
Engineering, Sciences and Technology, Topi 23-640, Pakistan

M.-t. Hyun
Department of Mechanical Engineering, Jeju National University,
Jeju 690-756, Korea

continuous and drop-on-demand mode can produce micro or even nanosize patterns. Many researchers have focused on the continuous mode of electrohydrodynamic jet printing through a stable cone-jet mode for the patterning purpose using various materials in electronics [16] and bioapplications [17]. However, this micro or nanosize high speed jet is difficult to stabilize [18]. Researchers have suggested different methods [19] and nozzle shapes [20] for stabilization of the jet. Moreover, patterns through the continuous jet mode may break or become irregular with a bead-like structure due to capillary forces or evaporation of the solvent or concentration of the suspension particles [21].

In order to address these issues, deposition through the drop-on-demand mode has been suggested by applying the pulse voltage. Park et al. [22] reported high resolution electrohydrodynamic jet printing at the submicron level using gold coated glass capillaries. Electrohydrodynamic drop-on-demand printing is performed by applying the pulsed voltage to the liquid and has been employed in electronics [22] and bioapplications [23]. Li [24] has studied drop-on-demand phenomena through meniscus deformation by applying the pulsed voltage. Stachewicz et al. [25] explained the drop-on-demand behavior using relaxation times and operating conditions. Lei et al. [26] explained the dependency of the droplet deposition frequency with respect to flow-rate, applied voltage, and pulse time using a polymeric solution. For direct patterning of the conductive tracks, Choi et al. [27] demonstrated the droplet deposition of the silver nanoparticles by applying pulse voltage; however, the deposited droplet was larger than the nozzle size. Park et al. [22] has demonstrated the printing of less than 10 μm patterns of PEDOT:PSS on 300 nm layers of SiO_2 on the conductive Si substrate. Wang et al. [28, 29] deposited Au and Ag nanoparticles on conductive silicon with a feature size of less than 10 μm and 35 μm by controlling through pulse voltage. Kim et al. [30] and Rahman et al. [31] deposited ink containing Cu and Ag nanoparticles, respectively, on the thick glass substrate by applying forward multistep wave form or multistep pulse voltage. For the requirement of printed electronics device fabrication, conductive patterns or active materials have to be deposited on glass and thick polymer substrates. But this is the one of the major limitations of electrohydrodynamic jet printing in the continuous mode due to the charge carried by an electrified jet, which affects the stability of the jet and also resolution of the printed patterns. The electrohydrodynamic printing in drop-on-demand mode is the more suitable choice for patterning on the thick substrate, because of event based formation of the cone-jet, which helps in a more stable printing process, and can produce a smaller diameter droplet than the nozzle size. However, fine resolution of Ag patterns less than 10 μm on the thick substrate has not been reported previously.

This paper presents the direct fabrication of less than 10 μm Ag patterns on a 500 μm thick glass substrate by

applying the pulse voltage with the frequency of 250 Hz using a 10 μm internal diameter glass capillary. The deposition frequency is studied by deposition position of the droplet on glass substrate and substrate speed. The effect on droplet size is studied with respect to operating parameters such as applied voltage, pulse time (1msec to 3 msec), and applied pressure. The droplet size is measured after the sintering process. Continuous patterns are printed by sufficient overlapping the deposited droplets by adjusting the substrate speed. The electrical functionality of continuous patterns is measured through the I–V curve.

2 Experimental setup

Figure 1 shows the schematic of the experimental setup used for electrohydrodynamic jet printing. The glass capillary with an internal diameter of 10 μm (World Precision Instruments) was connected with ink reservoir which was mounted on manual z-stage to adjust the gap between nozzle and substrate. For the ink supply to the nozzle tip, the ink reservoir was connected with the pressure regulator by maintaining the steady and constant flow-rate through compressed air. The pulsed voltage was applied through a metallic wire, which was inserted in a glass capillary and connected with a high voltage power amplifier (Trek 610E) and controlled with a multifunction signal synthesizer (HP 33120A). The droplets and patterns were deposited on a 500 μm thick 10 cm \times 10 cm glass substrate without any surface treatment, placed on the top of a ground electrode plate. The ground plate was mounted on X–Y motorized stage (SURUGA SEIKI DS102) to control the substrate speed during the patterning process. The nozzle to glass substrate distance was set at 250 μm for deposition of Ag nanoparticles. For

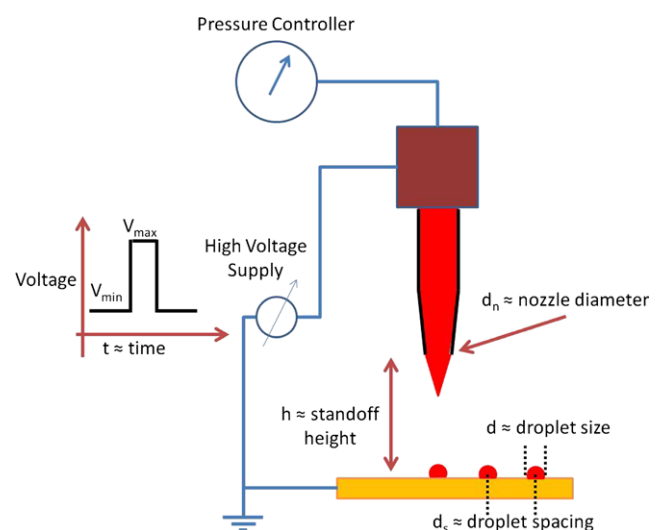


Fig. 1 Schematic diagram of experimental setup used for electrohydrodynamic patterning by applying pulse voltage

patterning, commercially available 55 wt% Ag nanoparticles ink having a surface tension of 23.3 mNm, viscosity of 10.9 mPa.s, and specific gravity of 1.64 gm/ml was used to be ejected from the glass capillary. The deposition process on the substrate was observed with a high speed camera (Motion Pro X3). After sintering the printed droplets and patterns at 150 °C for 60 minutes, dimensions were measured through a digital microscope (Olympus BX51M) and electrical characterizations were performed by measuring the I–V curve (Agilent B1500A). The wetting of the ink on the untreated glass substrate was measured with the help of the contact angle analyzer (Phoenix 300). The measured contact angle was 110 for Ag ink with the glass substrate, which shows the hydrophilic nature and spreading of the droplet.

3 Results and discussions

3.1 Droplet size and operating conditions

Initially, experiments were performed to investigate the minimum bias voltage (V_{\min}) and pulse voltage (V_{\max}) by applying 250 Hz frequency and 2 msec of pulse time with constant pressure of 1 kPa for stable generation of a droplet of Ag nanoparticles on a glass substrate. The effect of the operating conditions was measured with the help of the droplet diameter after the sintering process. It was noted that minimum droplet diameter of 18 μm with the deviation of $\pm 0.5 \mu\text{m}$ was measured at V_{\min} of 1000 V and V_{\max} 1750 V, with center to center distance of $100 \mu\text{m} \pm 5 \mu\text{m}$ between two neighboring droplets, as shown in Fig. 2. With a further increase in V_{\min} , small droplets are ejected before ejecting the primary droplet as shown in Fig. 3. This is due to the high V_{\min} causing the jetting in prior to application of droplet generation pulse voltage (V_{\max}). As in the case of increasing V_{\max} from 1750 V to 1800 V and keeping the value of V_{\max} at 1000 V, irregular droplets surrounding with smaller atomized droplets were generated as shown in Fig. 4. In both of the cases with a high value of V_{\max} and V_{\min} droplets on the substrate irregular due to disintegration of the droplet before reaching the substrate because of excess charges are carried by droplets at high applied voltages [32].

The droplet generation behavior and droplet diameter with respect to pulse time is shown in Fig. 5. As shown in the graph, at the same applied voltage, the droplet size is proportional to the applied pulse time. The droplet diameter measured by applying 1 msec of pulse time at V_{\min} of 1000 V and V_{\max} of 1750 V, was approximately 8 μm and at 3 msec of pulse time, the droplet diameter is measured to be 37 μm . This change in droplet diameter is related with the ejection volume during the drop-on-demand jetting; the ejection volume increases with respect to increase in pulse

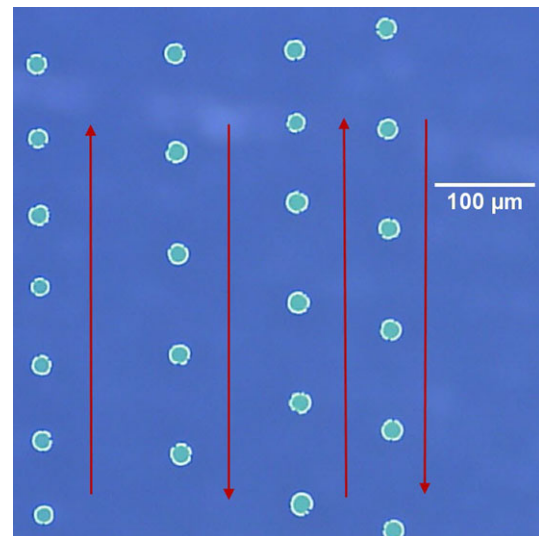


Fig. 2 Droplet diameter of 18 μm with the deviation of $\pm 0.5 \mu\text{m}$ at V_{\min} of 1000 V and V_{\max} 1750 V, with droplet spacing of $100 \mu\text{m} \pm 5 \mu\text{m}$ (arrows indicating the direction of printing)

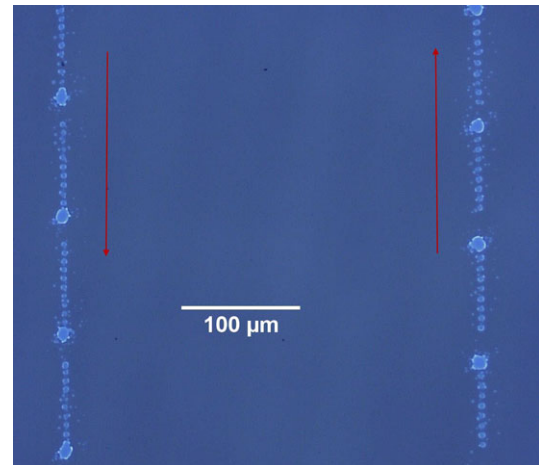


Fig. 3 Droplet generation when V_{\min} of 1050 V, V_{\max} 1750 V, 2 msec of pulse time, and 1 kPa of applied pressure; smaller droplets were generated before main droplet generation due to high value of V_{\min} (red arrow indicating the direction of printing)

time of applied ejection voltage [33]. However, change in the droplet diameter with respect to the applied voltage is approximately 15 %. In the electrohydrodynamic jetting, the effect on droplet size of the jet is less as compared to the liquid flow-rate [34].

After investigating the voltage range for stable deposition of Ag nanoparticles droplets, the effect of applied pressure is investigated by applying 250 Hz frequency with V_{\min} of 750 V and V_{\max} of 1500 V at 1 msec to 3 msec is shown in Fig. 6. The minimum pressure at which steady drop-on-demand behavior observed was 0.5 kPa. Under 0.5 kPa of applied pressure, the droplet generation frequency was smaller than the applied voltage frequency. This behavior was due to the in-

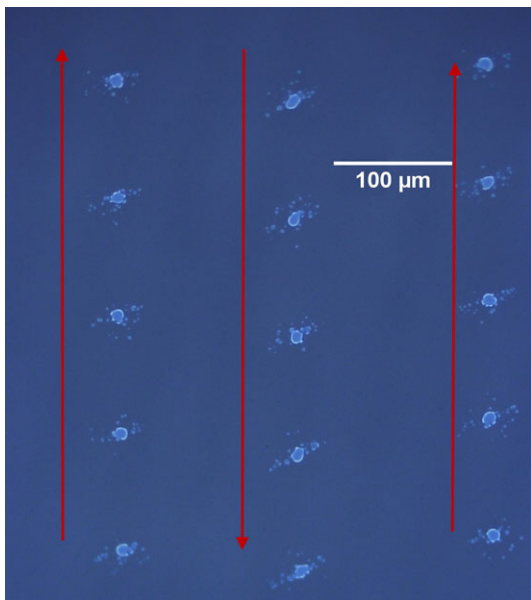


Fig. 4 Irregular droplet with smaller droplets surrounding the main droplet generation when V_{\min} of 1000 V, V_{\max} 1800 V, 2 msec of pulse time, and 1 kPa of applied pressure due to high value of V_{\max} (red arrow indicating the direction of printing)

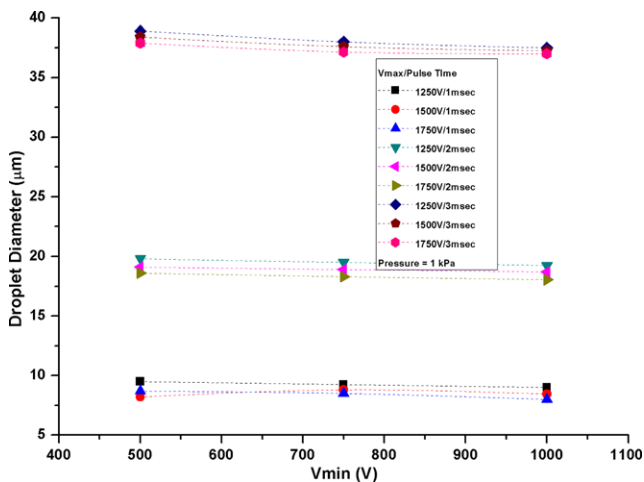


Fig. 5 Droplet diameter with respect to V_{\min} at different V_{\max} and pulse time

sufficient supply of ink at the tip of the nozzle which affects the droplet generation frequency [26]. It was observed that the droplet diameter increases with an increase in applied pressure due to an increase in the liquid supply. This shows that the size of the droplet diameter is more dependent on applied pressure as compared to applied voltage, which can be used for controlling the droplet size deposition on the substrate. In case of the pressure effect on the droplet size, the minimum droplet diameter achieved was 3.8 μm at 0.5 kPa, V_{\min} 750 V, and V_{\max} of 1500 V with a pulse time of 1 msec. At high pressure and pulse time, the droplet frequency

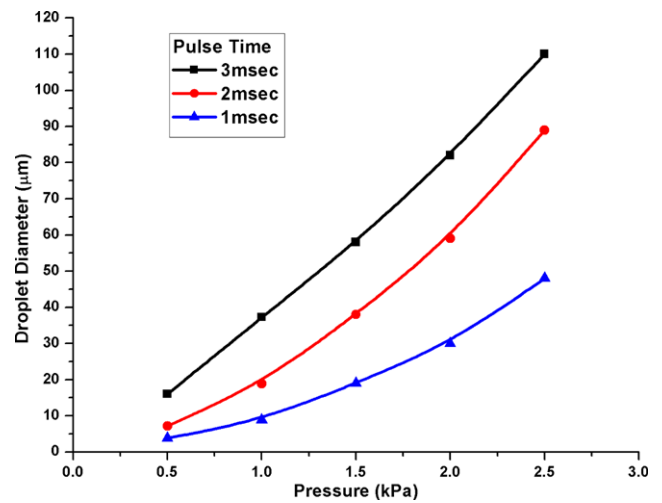


Fig. 6 Droplet size dependency on applied pressure at 250 Hz frequency with V_{\min} 750 V and V_{\max} 1500 V at different applied pulse time

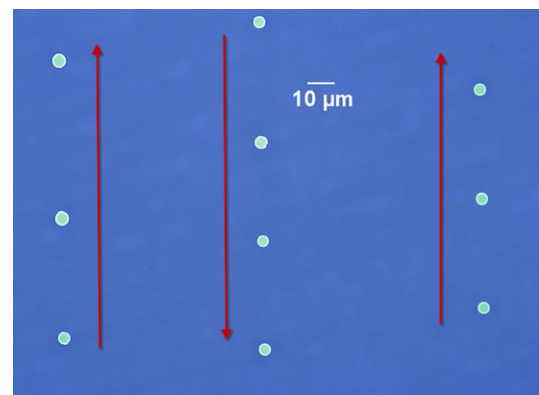


Fig. 7 Droplet diameter of 3.6 μm by applying V_{\min} 900 V, V_{\max} 1600 V, 1 msec pulse time, and applied pressure 0.5 kPa (red arrow indicating the direction of printing)

and size was difficult to measure because of the overlapping of the large diameter droplet at 25 mm/sec substrate speed.

In order to minimize the droplet size at 0.5 kPa applied pressure, the droplet diameter was measured by increasing the applied pulsed voltage at 250 Hz frequency with a pulse time of 1 msec. The minimum droplet diameter of 3.6 μm was measured after the sintering process at V_{\min} of 900 V and V_{\max} 1600 V as shown in Fig. 7. The SEM image of the 3.6 μm after the sintering process is shown in Fig. 8. The droplet diameter was also investigated by increasing pulse time and results are compared with the droplet diameter with V_{\min} of 750 V and V_{\max} of 1500 V at the corresponding pulse time, as shown in Fig. 8. As shown in the graph at Fig. 9, the effect of the applied voltage is not significant as compared to the pulse time on the droplet diameter. At V_{\min} of 750 V, V_{\max} 1500 V, and 1 msec pulse time, the droplet diameter is 5.2 times smaller than the droplet generated at same voltage and pulse time of 3 msec. However, when the

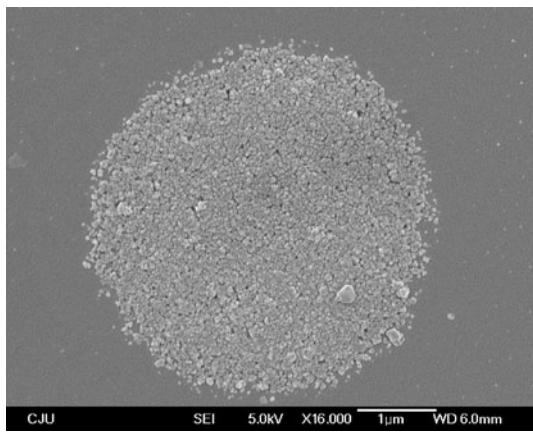


Fig. 8 SEM image of 3.6 μm after sintering process

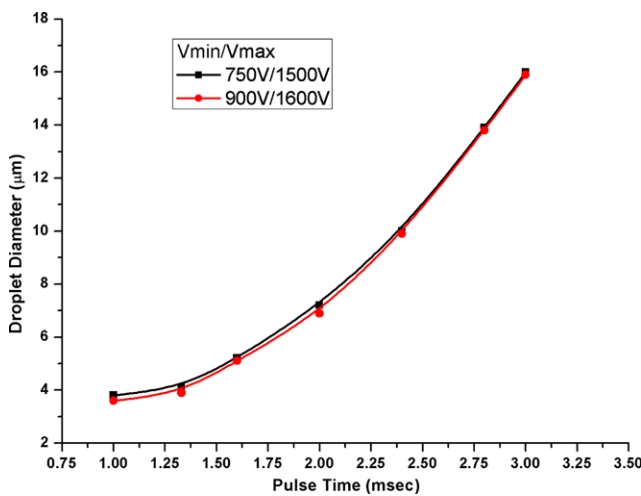


Fig. 9 Comparison of droplet diameter between applied voltages at different pulse time, red line V_{min} 900 V, V_{max} 1600 V, and black line V_{min} 1750 V, V_{max} 500 V, constant pressure was kept at 0.5 kPa

V_{min} of 950 V, V_{max} 1600 V, and 1 msec pulse time was applied, the droplet size is only increased by approximately 0.6 %.

The experimental results indicate that in drop-on-demand phenomena, at any given frequency, the dependency of the droplet size is more on applied pressure and pulse time as compared to applied voltages.

3.2 Printing of continuous patterns

For direct deposition of Ag conductive tracks on the substrate, the patterns are formed by overlapping of the consecutive droplets by adjusting the substrate speed [35] with respect to droplet frequency and size. Figure 10 shows the high speed image of the patterning process on the glass substrate. A number of experiments were performed to investigate the optimal substrate speed to produce smooth patterns of Ag nanoparticles, with a droplet frequency of 250 Hz by

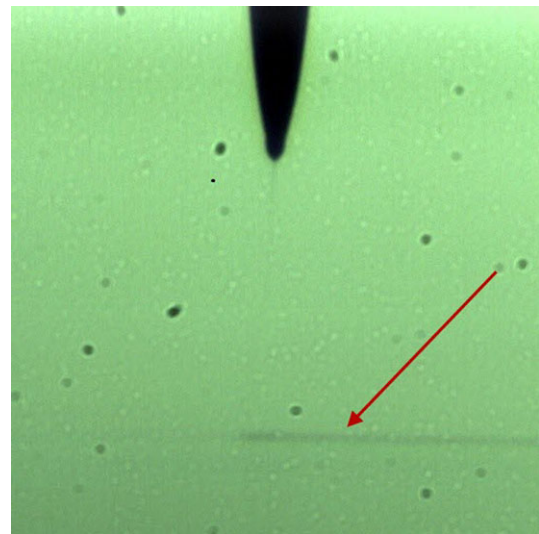


Fig. 10 Printing process of the continuous conducting pattern of Ag nanoparticles on glass substrate, where red arrow indicates the printing patterns

applying V_{min} of 900 V and V_{max} of 1600 V at the pulse time of 1 msec with an applied pressure of 0.5 kPa, whereas the droplet diameter was 3.6 μm on the glass substrate. It was noted that when the substrate speed is relatively high and distance between the consecutive droplets is slightly smaller than the droplet diameter, the drop coalescence was observed, which caused irregular patterns with beads. However, at a very low substrate speed, where the droplet spacing is relatively smaller, the patterns were formed with bulging instability. It was noted that, when the distance between consecutive droplets was approximately 70 % of the droplet diameter, the smooth patterns with no beads or bulging were formed. Figure 11 shows the effect of the substrate speed or distance between the consecutive droplets for 3.6 μm droplets. As shown in Fig. 11(a), irregular patterns with beads are formed when distance between the consecutive droplets is 90 % of the droplet diameter, when the distance was approximately 70 % of the droplet diameter, smooth and regular patterns of 6.5 μm approximate width (1.8 times larger than the printed droplet size) were formed as shown in Fig. 11(b) and Fig. 11(c) shows patterns with bulging instability due to droplet spacing, which was 50 % of the droplet diameter. Based on the experiment results, for smooth patterns substrate speed (V_s) with respect to droplet size (d) and droplet generation frequency (f_d) can be predicted as:

$$V_s = f_d * 0.7d \tag{1}$$

However, experimental results also indicated that for stable and a smooth pattern generation through larger droplets, the center-to-center distance between the consecutive droplets had to be kept larger than 70 % of the droplet diameter. The printed pattern width according to printed droplet size is shown in Fig. 12, where the droplet frequency of 250 Hz

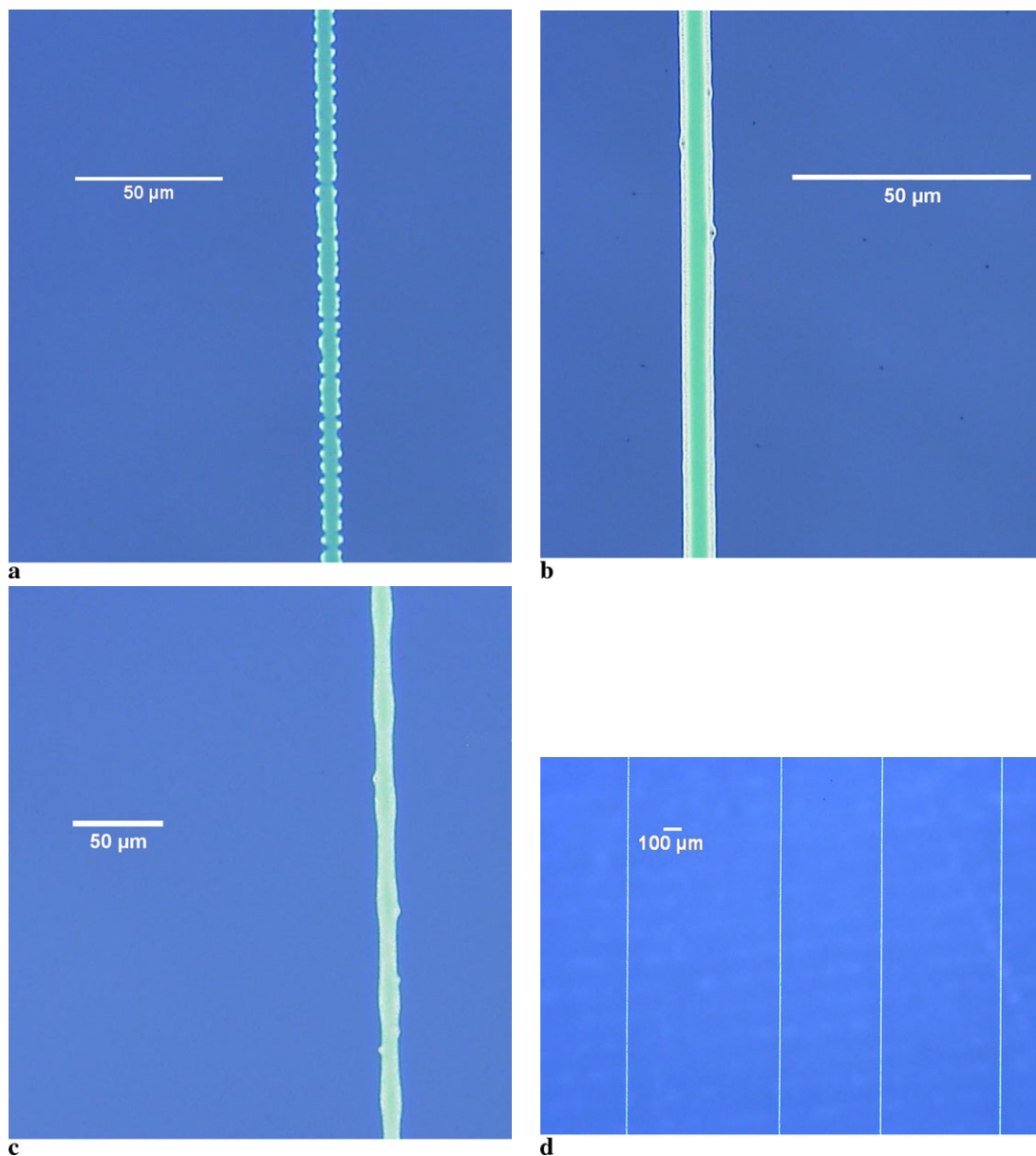


Fig. 11 Droplets overlapping by controlling substrate (droplet diameter 3.6 μm), **(a)** irregular patterns with beads droplets spacing is 90 % of the droplet diameter, **(b)** smooth pattern of 6.5 μm width with droplet spacing is 70 % of the droplet diameter **(c)** shows patterns with

bulging instability due to droplet spacing was 50 % of droplet diameter, and **(d)** microscopy image consecutive patterns of 6.5 μm on glass substrate after sintering process

by applying V_{min} of 900 V and V_{max} of 1600 V with applied pressure of 0.5 kPa, by changing pulse time. Figure 13 shows the patterns by overlapping 7, 11, and 13 μm droplets and the patterns size are approximately 16, 20, and 25 μm , respectively.

The electrical characterization was measured through I–V data, by connecting 2 probes on the sintered printed sliver patterns at the distance of 2 mm after the sintering process. The change in current was measured by increasing the voltage, which showed linear Ohmic behavior. The re-

sistance of 6.5, 12.6, and 31.3 μm patterns were measured to be 111, 85, 62.5 Ω , respectively. The electrical characterization results shows that the fine resolution patterns printed through electrohydrodynamic printing can be used to fabricate conductive tracks for printed electronics application.

4 Conclusions

Fine resolution Ag nanoparticles patterns are successfully deposited on untreated thick glass substrates using electro-

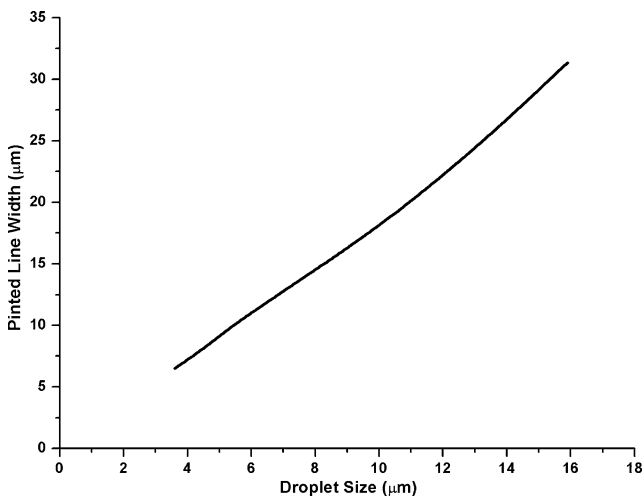


Fig. 12 Change in pattern width with respect to droplet diameter; maintaining the droplet spacing of 70 % of droplet diameter by applying V_{\min} 900 V and V_{\max} 1600 V with applied pressure of 0.5 kPa by changing pulse time from 1 msec to 3 msec.

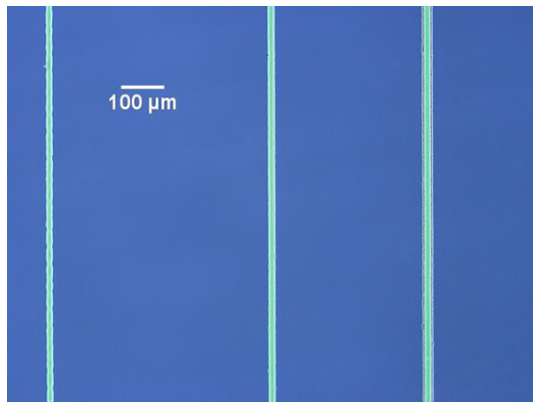


Fig. 13 Printing of smooth patterns with respect to droplet size, 16 µm patterns formed by overlapping approximately 7 µm droplets (*left*), 20 µm patterns formed by overlapping approximately 11 µm droplets (*center*), and 25 µm patterns formed by overlapping approximately 13 µm droplet (*right*)

hydrodynamic jet printing in drop-on-demand mode, which is the main benefit of this direct patterning technology over other convention inkjet patterning to produce very small droplets than the nozzle size. The experiment results indicate that printed droplet size at any given frequency is depended on the operating conditions; applied voltage, pulse time, and pressure. However, the applied pressure and pulse time have a more prominent effect on the droplet size as compared to applied voltage. Continuous patterns were fabricated by overlapping consecutive droplets by adjusting the substrate speed with respect to the droplet diameter. For smooth and continuous patterns, the experiment results revealed that 70 % of droplet spacing is sufficient, for given experiment setup. I–V curves of the sintered printed patterns showed linear Ohmic behaviors. The minimum droplet

diameter achieved 3.6 µm, where as the pattern width was approximately 6.5 µm, which is 2.7 and 1.53 times smaller than the nozzle internal diameter, respectively, which highlights the main advantage of electrohydrodynamic printing to produce a smaller pattern size as compared to the nozzle diameter. This feature of electrohydrodynamic printing of conductive patterns can help in miniaturizing the electronics devices using noncontacting direct printing technology.

Acknowledgements This research was supported by Basic Science Research Program through the National Research Foundation of Korea (NRF) funded by the Ministry of Education, Science and Technology (2010-0026163) and the research grant by Jeju National University in 2010.

References

1. D.B. Chrisey, *Science* **289**, 879–881 (2000)
2. B.J. Gans, P.C. Duineveld, U.S. Schubert, *Adv. Mater.* **16**, 203–213 (2004)
3. T. Shimoda, Y. Matsuki, M. Furusawa, T. Aoki, I. Yudasaka, H. Tanaka, H. Iwasawa, D. Wang, M. Miyasaka, Y. Takeuchi, *Nature* **440**, 783–786 (2006)
4. J.B. Szczech, C.M. Megaridis, D.R. Gamota, J. Zhang, *IEEE Trans. Electron. Packag. Manuf.* **25**, 26–33 (2002)
5. A. Bietsch, M. Hegner, H.P. Lang, C. Gerber, *Langmuir* **20**(12), 5119–5122 (2004)
6. P. Calvert, *Chem. Mater.* **13**, 3299–3305 (2001)
7. B. Derby, *Annu. Rev. Matter. Res.* **40**, 395–414 (2010)
8. K. Cheng, M.H. Yang, W.W. Chiu, C.Y. Huang, T.F. Ying, Y. Yang, *Macromol. Rapid Commun.* **26**, 247 (2005)
9. G. Taylor, *Proc. R. Soc. Lond. A* **280**, 383–397 (1964)
10. H.F. Poon, D.A. Saville, I.A. Aksay, *Appl. Phys. Lett.* **93**, 133114 (2008)
11. G.S. Bisht, G. Canton, A. Mirsepassi, L. Kulinsky, S. Oh, D. Dunn-Rankin, M.J. Madou, *Nano Lett.* **11**(4), 1831–1837 (2011)
12. A. Khan, K. Rahman, M.T. Hyun, D.S. Kim, K.H. Choi, *Appl. Phys. A, Mater. Sci. Process.* **104**(4), 1113–1120 (2011)
13. Z. Huneiti, W. Machowski, W. Balachandran, in *IEEE 31th IAS Annual Meeting, San Diego*, vol. 3 (1996), pp. 1768–1774
14. R. Juraschek, F.W. Rollgen, *Int. J. Mass Spectrom.* **177**, 1–15 (1998)
15. J.H. Kim, H.C. Oh, S.S. Kim, *J. Aeronaut. Sci.* **39**(9), 819–825 (2008)
16. D.Y. Lee, E.S. Hwang, T.U. Yu, Y.J. Kim, J. Hwang, *Appl. Phys. A* **82**, 671–674 (2006)
17. Z. Ahmad, J. Huang, E.S. Thian, M.J. Edirisinghe, S.N. Jayasinghe, S.M. Best, W. Bonfield, R.A. Brooks, N. Rushton, *J. Biomed. Nanotechnol.* **4**, 185–195 (2008)
18. M.M. Hohman, M. Shin, G. Rutledge, M. Brenner, *Phys. Fluids* **13**, 2201–2220 (2001)
19. S. Korkut, D.A. Saville, I.A. Aksay, *Phys. Rev. Lett.* **100**(3), 034503 (2008)
20. S.Y. Kim, Y. Kim, J. Park, J. Hwang, *J. Micromech. Microeng.* **20**, 55009 (2010)
21. S. Korkut, D.A. Saville, I.A. Aksay, *Langmuir* **24**, 12196–12201 (2008)
22. J.U. Park, M. Hardy, S.J. Kang, K. Barton, K. Adair, D.K. Mukhopadhyay, C.Y. Lee, M.S. Strano, A.G. Alleyne, J.G. Georgiadis, P.M. Ferreira, J.A. Rogers, *Nat. Mater.* **6**, 782–789 (2007)
23. J.U. Park, J.H. Lee, U. Paik, Y. Lu, J.A. Rogers, *Nano Lett.* **8**(12), 4210–4216 (2008)

24. J.L. Li, *J. Elast.* **65**, 750–757 (2007)
25. U. Stachewicz, J.F. Dijksman, B. Burdinski, C.U. Yurteri, J.C.M. Marijnissen, *Langmuir* **25**, 2540–2549 (2009)
26. L. Xu, X. Wang, T. Lei, D. Sun, L. Lin, *Langmuir* **27**(10), 6541–6548 (2011)
27. J. Choi, Y.J. Kim, S. Lee, S.U. Son, H.S. Ko, V.D. Nguyen, D. Byun, *Appl. Phys. Lett.* **93**, 193508 (2008)
28. K. Wang, J.P.W. Stark, *J. Nanopart. Res.* **12**(3), 707–711 (2010)
29. K. Wang, J.P.W. Stark, *Appl. Phys. A, Mater. Sci. Process.* **99**, 763–766 (2010)
30. D.S. Kim, A. Khan, K. Rahman, S. Khan, H.C. Kim, K.H. Choi, *Mater. Manuf. Process.* **26**(9), 1196–1201 (2011)
31. K. Rahman, A. Khan, N.M. Nam, K.H. Choi, D.S. Kim, *Int. J. Prec. Eng. Manuf.* **12**(4), 663–669 (2011)
32. H.T. Yulistira, V.D. Nguyen, P. Dutta, D. Byun, *Appl. Phys. Lett.* **96**, 023503 (2010)
33. U. Stachewicz, J.F. Dijksman, C.U. Yurteri, J.C.M. Marijnissen, *Microfluid. Nanofluid.* **9**, 635–644 (2010)
34. A.M. Gafian-Calvo, J. Davila, A. Barrero, *J. Aerosol Sci.* **28**(2), 249–275 (1997)
35. J. Stringer, B. Derby, *Langmuir* **26**(12), 10365–10372 (2010)